Scientific Research Publishing

Energy and Power Engineering, 2022, 14, 181-200
https://www.scirp.org/journal/epe
ISSN Online: 1947-3818
ISSN Print: 1949-243X

Assessment of the Wind Energy Potential of Two Burundian Sites

Mathias Bashahu[1*], Pierre Nsabimana[1], Juvenal Barakamfitiye[2], Fidele Niyukuri[2]

[1]Department of Physics and Technology, University of Burundi, Bujumbura, Burundi
[2]Department of Mathematics, Institute of Applied Pedagogy, University of Burundi, Bujumbura, Burundi
Email: *bashahuma@yahoo.fr

How to cite this paper: Bashahu, M., Nsabimana, P., Barakamfitiye, J. and Niyukuri, F. (2022) Assessment of the Wind Energy Potential of Two Burundian Sites. *Energy and Power Engineering*, **14**, 181-200.
https://doi.org/10.4236/epe.2022.145010

Received: February 21, 2022
Accepted: May 28, 2022
Published: May 31, 2022

Abstract

1-year hourly wind speed data from two Burundian stations, namely Bujumbura and Muyinga, have been processed in this work to bring an efficient help for the planning and installation of wind energy conversion systems (WECS) at those localities. Mean seasonal and diurnal variations of wind direction and wind shear exponent have been derived. Two-parameter Weibull probability density functions (PDFs) fitting the observed monthly and annual wind speed relative frequency distributions have been implemented. As shown through three complementary statistical tests, the fitting technique was very satisfactory. A wind resource analysis at 10 m above ground level (AGL) has led to a mean power density at Bujumbura which is almost thirteen fold higher than at Muyinga. The use of the empirical power law to extrapolate wind characteristics at heights from 150 to 350 m AGL has shown that energy potential of hilltops around Muyinga was only suitable for small, individual scale wind energy applications. At the opposite, wind energy potential of ridge-tops and hilltops around Bujumbura has been found suitable for medium and large scale electricity production. For that locality and at those heights, energy outputs and capacity factors (*CF* or C_f) have been computed for ten selected wind turbines (WTs), together with costs of electricity (*COE*) using the present value of cost (*PVC*) method. Amongst those WTs, YDF-1500-87 and S95-2.1 MW have emerged as the best options for installation owing to their highest *CF* and lowest *COE*. Moreover, an analysis of those two quantities at monthly basis for YDF-1500-87 WT has led to its best performance in the dry season. Compared to the average present *COE* of household hydroelectricity consumption, results of this study have evidenced economical feasibility and benefit of WECS setting in selected Burundian sites in order to supplement traditional electricity sources.

Keywords

Wind Shear Exponent, Two-Parameter Weibull PDFs, Statistical Tests,

Wind Energy Potential, WT's Energy Output and Capacity Factor, Cost of Electricity, Two Burundian Sites

1. Introduction

Almost 98% of the population in Burundi still uses firewood or wood scraps in rural areas and charcoal in urban zones for their main energy needs, which are food cooking, house heating and lighting. In average, less than 5% of that population has access to electricity (with 2% in the rural areas and 52% in the urban ones) [1]. 98.2% of the total electricity consumption (400 GW-hr; 2014's estimate) comes from hydroelectric plants and 1.8% from fossil fuels [2]. The average annual electricity consumption is less than 30 kWh per capita, which is almost five fold lower than the average one in Africa. The electricity production (300 GW-hr; 2014's estimate) is inadequate when it faces up to an increasing energy demand due to industrialization effort and to a high rate of population growth (3.26%; on a total population of 11,099,298; 2016's estimate) [2]. That feature is well illustrated by electricity shortages frequently observed daily in different urban areas. As a consequence and in order to bypass such events, besides country electricity imports (100 GW-hr; 2014's estimate) [2], various firms, institutions or departments resort to motor generators such as Diesel engines, which use imported fossil fuels, particularly refined petroleum products. Like in many other countries, effort is nowadays made in Burundi to increase electricity production and to alleviate the constantly scaling cost and environmental concern of fossil fuels. One way to achieve those objectives and which is clearly stated in the current government's working agenda [1] [3] [4], is to supplement traditional energy sources with free, clean and inexhaustible energy sources, particularly the solar and the wind energy ones.

The present work deals with the possible use of wind energy source in Burundi. An essential stage for that purpose is the selection of the most suitable site to settle a wind energy conversion system (WECS) and the decision about the system's parameters (e.g.: blade shape and size, direction, total capacity, etc.). That requires a good knowledge of various properties of the site and those properties should be found out by using not only wind dynamic and statistical data [5] [6], but also data about climate, e.g.: air density, temperature, humidity, pressure [7] [8], land topography, obstacles and surface roughness [9] [10]. Research papers in that context for Burundian sites are rather scarce, but one should mention a recent study which compares the effectiveness of different PDFs in fitting experimental frequency distributions of wind speed data [11]. The major aim of this work is to provide decision makers with a technical study which should bring an efficient help for the planning and implementation of WECS projects at two Burundian localities, namely Bujumbura and Muyinga. For that purpose, hourly wind speed data recorded over a 1-year period at those sites have been processed

and validated models have been used to extrapolate different wind energy potential statistical characteristics. Moreover, through the computation of energy output, capacity factor and cost of electricity per unit energy output, the performance of some wind machines for electricity production at different tower hub heights has been also assessed.

2. Materials and Methodology

2.1. Sites and Basic Data

As an African country with a total (land and water) area of 27,834 km^2 and a population density of 432.22 persons per km^2 [2], Burundi is located closely to the equatorial zone, at latitudes (φ) between 2˚10'S and 4˚30'S, and longitudes (L) between 28˚50'E and 30˚53'E. Long-term records of the wind speed and wind direction have been performed at different stations and then collected and kept within the Geographical Institute of Burundi (IGEBU). The records were made daily between 6:00 and 18:00 local time (LT) by the means of an anemometer fitted with an integrating device. Proper calibration of that device allowed the derivation of wind speed data (v, in m/s) averaged over a 1-hour or 3-hour period. For most of the stations, wind speed measurements were referred to 2 m height above the ground level (AGL). Exceptionally, wind speed data were available at 2 m and 12 m AGL for only two stations, namely Bujumbura (airport; L = 29˚21'E; φ = 3˚23'S; z' = 783 m) and Muyinga (airport; L = 30˚21'E; φ = 2˚51'S; z' = 1755 m), which are shown in **Figure 1**. The quantity z' is the altitude of the station.

The measured hour-by-hour wind speed data used to implement Weibull distributions of section 2.2 refer to 12 m height AGL at the two previous sites and to a 1-year period of continuous records with a minimum number of missing data. Moreover, the wind shear exponent (α) data quoted in section 2.3 have been derived from wind speed measurements at heights z_1 = 2 m and z_2 = 12 m AGL for any of the two sites, together with the next expression extracted from the common empirical power law [9] [12] [13] [14] [15] [16]:

$$\alpha = \frac{\ln\left(\frac{v_2}{v_1}\right)}{\ln\left(\frac{z_2}{z_1}\right)} \tag{1}$$

2.2. Weibull Distributions Fitting the Observed Frequency of Wind Speed Data

2.2.1. Fitting Technique

Efforts have been made to fit field data of wind speed as well as wind power and energy densities with different standard mathematical functions playing the role of frequency distributions. Beside other distributions including notably the Pearson VI, exponential, gamma, logistic and Rayleigh ones, the two-parameter Weibull distribution is widely used for wind data analysis. It is described by the

Figure 1. Geographical position of the two sites of this study.

following cumulative distribution function (CDF), $F(v)$ and probability density function (PDF), $f(v)$ of observing wind speed v [5] [13] [17]:

$$F(v)=1-\exp\left[-\left(\frac{v}{c}\right)^{k}\right] \tag{2}$$

and

$$f(v)=\frac{\mathrm{d}F}{\mathrm{d}v}=\frac{k}{c}\left(\frac{v}{c}\right)^{k-1}\exp\left[-\left(\frac{v}{c}\right)^{k}\right] \tag{3}$$

where c and k are the Weibull scale parameter (m/s) and modulus or shape parameter (dimensionless), respectively. The different techniques quoted in the literature to estimate the two previous parameters include notably the graphical method, maximum likehood method, modified maximum likehood method, standard deviation method, power density method, moments method, equivalent energy method, Justus's empirical method, Lysen's empirical method [5] [6] [7] [18] [19] [20] and median rank regression method [21]. In the present study, once the mean ($\overline{v}$) and variance (σ^2) of the observed wind speed frequency distribution were known, the following relationships have been used to determine the Weibull shape and scale parameters [22] [23]:

$$k=\left(\frac{\sigma}{\overline{v}}\right)^{-1.086},\quad 1\le k\le 10 \tag{4}$$

and

$$c=\frac{\overline{v}}{\Gamma\left(1+\frac{1}{k}\right)} \tag{5}$$

where $\Gamma(x)$ is the gamma function of a real variable x, for which values are available in tables [24].

2.2.2. Tests of the Effectiveness of the Fitting Technique

The effectiveness of the fitting technique has been checked through the next three complementary statistical tests which have demonstrated their usefulness in other works [25] [26] [27] [28]: the mean bias error (*MBE*), root mean square error (*RMSE*) and *t*-statistics. They are respectively defined as:

$$MBE = \frac{1}{n}\left[\sum_{i=1}^{n}\left(f_{i,th} - f_{i,obs}\right)\right] \tag{6}$$

$$RMSE = \left[\frac{1}{n}\sum_{i=1}^{n}\left(f_{i,th} - f_{i,obs}\right)^2\right]^{1/2} \tag{7}$$

and

$$t = \left\{(n-1)(MBE)^2 \Big/ \left[(RMSE)^2 - (MBE)^2\right]\right\}^{1/2} \tag{8}$$

where $f_{i,obs}$ represents values of the observed relative frequency distribution of a given wind speed data set, $f_{i,th}$ indicates the counterparts of those values in the Weibull PDF fitting that distribution, and n is the total number of ranges with equal widths into which the previous data set has been divided. In those tests, a low *MBE* is expected. The smaller the *RMSE* is, the better the model's performance. Moreover, the Student's variable, t has to be compared to its critical value, $t_c = t(n-1,\alpha')$ at α' level of significance (or $\gamma = 1-\alpha'$ confidence level) and $n-1$ degrees of feedom, by reading statistical tables [29] [30]. The differences between $f_{i,th}$ and $f_{i,obs}$ were judged not statistically significant at a given confidence level ($\gamma = 99.5\%$ in this study) when the next condition was satisfied:

$$t < t_c \tag{9}$$

2.3. Wind Speed and Weibull Parameters Variation with Height

As the values of average wind speed and power density increase with height, higher WT tower hub heights are preferred to obtain higher wind energy densities. In this study, the empirical power law has been used to extrapolate the wind speed variation with height. It is expressed as

$$v = v_0\left(\frac{z}{z_0}\right)^{\alpha} \tag{10}$$

where v is wind speed estimated at a given height, z; v_0 is wind speed at reference height, z_0; and α is the ground surface friction coefficient, also called power law exponent or wind shear exponent. In several works, the reference height is $z_0 = 10$ m AGL as recommended by the World Meteorological Organization (WMO) [5]. The exponent α varies with height, time of day, season, nature of the terrain, wind speed and temperature. For the period and the two sites of this study, the use of the field data quoted at the end of Section 2.1 has led to the annual mean value $\alpha = 0.25$. Owing to Equations (4)-(5), for relatively low heights AGL, the shape parameter (k) remains almost constant when the height increases, while the scale parameter (c) varies with height at the same rate as the wind

speed (v).

2.4. Wind Power and Energy Content

Following the WD, different characteristics of the wind power and energy content are described in this section.

The average wind power density, $\overline{p}$ (in W/m^2) is given by the next relationship [9] [10] [12] [23]:

$$\overline{p} = \frac{1}{2}\rho c^3 \Gamma\left(1+\frac{3}{k}\right) = \frac{1}{2}\rho\left\{\frac{\overline{v}^3 \Gamma\left(1+\frac{3}{k}\right)}{\left[\Gamma\left(1+\frac{1}{k}\right)\right]^3}\right\} \tag{11}$$

where the mean air density, ρ, which depends on the site's altitude, air pressure and temperature, is usually taken as equal to 1.225 kg/m^3 [6] [29].

According to the Betz's limit, the average maximum wind power density which can be extracted from a WT is expressed as [6]:

$$\overline{p}_{\max} = 0.2963\rho c^3 \Gamma\left(1+\frac{3}{k}\right) \approx 59.3\%\,\overline{p} \tag{12}$$

Once the average wind power density of a site is known, the wind energy density for a given duration T (in hours) can be calculated (in W-hr/m^2) as [7] [10] [15]:

$$\overline{e} = \frac{1}{2}\rho c^3 \Gamma\left(1+\frac{3}{k}\right) T \tag{13}$$

At its turn, the wind energy pattern factor, E_{PF} is expressed as [9]:

$$E_{PF} = \frac{\overline{v^3}}{\overline{v}^3} = \frac{\Gamma\left(1+\frac{3}{k}\right)}{\left[\Gamma\left(1+\frac{1}{k}\right)\right]^3} \tag{14}$$

The most probable or most frequent wind speed, which refers to the maximum of the Weibull PDF, is given by the next relationship [6]:

$$v_{mp} = c\left(1-\frac{1}{k}\right)^{\frac{1}{k}} \tag{15}$$

while the optimum wind speed, or wind speed of maximum energy carrier, is expressed as [7] [15] [22]:

$$v_{op} = c\left(1+\frac{2}{k}\right)^{\frac{1}{k}} \tag{16}$$

2.5. Wind turbine energy output and capacity factor

In most cases, a WT operates at increasing power, $P_{CR}(v)$ between cut-in and rated wind speeds (v_C and v_R, respectively) and at constant rated power, P_R with maximum efficiency between rated and cut-off wind speeds (v_R and v_F, respec-

tively). Its power output performance curve, $P_T(v)$ is therefore described by the next relationship:

$$P_T(v) = \begin{cases} P_{CR}(v), & v_C \le v < v_R \\ P_R, & v_R \le v < v_F \\ 0, & v < v_C; v \ge v_F \end{cases} \tag{17}$$

Different WTs have different power output performance curves, so the models to describe those curves are different. For the function $P_{CR}(v)$ in particular, quadratic [12], cubic [15] and 3-degree polynomials [7] have been used, as well as various other expressions [5] [9] [10] [31].

Once the function $P_T(v)$ is known, the actual wind energy output from a WT over a given duration T (in hours) is calculated as [15]:

$$E_{TA} = T\int_0^{\infty} P_T(v) f(v) \mathrm{d}v = T\left[\int_{v_C}^{v_R} P_{CR}(v) f(v) \mathrm{d}v + \int_{v_R}^{v_F} P_R f(v) \mathrm{d}v\right] \tag{18}$$

where $f(v)$ is the actual site's wind speed PDF (Equation (3)).

In this work, a model WT is assumed with the quantities P_R, $P_T(v)$ and E_{TA}/T in Equations (17)-(18) representing the rated electrical power (P_{eR}), electrical power output (P_e) and average electrical power output ($P_{e,ave}$), respectively. The model is simulated using the next relationships [31] [32]:

$$P_{eCR}(v) = P_{eR}\left(\frac{v^k - v_C^k}{v_R^k - v_C^k}\right) \tag{19}$$

and

$$P_{e,ave} = \left\{\frac{\mathrm{e}^{-\left(\frac{v_C}{c}\right)^k} - \mathrm{e}^{-\left(\frac{v_R}{c}\right)^k}}{\left(\frac{v_R}{c}\right)^k - \left(\frac{v_C}{c}\right)^k} - \mathrm{e}^{-\left(\frac{v_F}{c}\right)^k}\right\} \tag{20}$$

where P_{eCR} represents the quantity $P_{CR}(v)$ of Equation (17). At its turn, the WT capacity factor, C_f is given by the ratio of the average electrical power output to the rated electrical power of the WT [15] [31] [32]:

$$C_f = \frac{P_{e,ave}}{P_{eR}} \tag{21}$$

2.6. Economic Analysis

Amongst the different ways of estimating the economics of WTs, the method used in this study is the specific cost per kW-hr of electrical energy generated by a WT, which is defined as the ratio of the present value of cost (PVC) to the energy output during the WT lifetime. The PVC is expressed as [10] [31] [32]:

$$PVC = I + C_{omr}\left(\frac{1+i}{r-i}\right)\left[1 - \left(\frac{1+i}{1+r}\right)^n\right] - S\left(\frac{1+i}{1+r}\right)^n \tag{22}$$

In that relationship, I is the investment cost of the WT (the price of the WT in addition with 20% for civil works and other connections). The prices of WTs

based on the rated power are indicated in Table 1. C_{omr} represents the operation, maintenance and repair costs (15% of I); S is the scrap value (10% of I); n is the WT lifetime (20 years) and the discount rate, r is expressed as:

$$r = \frac{i_0 - i}{1 + i} \tag{23}$$

where i_0 is the nominal interest rate (12%) and i represents the inflation rate (5%).

The total energy output over the WT lifetime (in kW-hr) is computed as:

$$E_{WT} = 8760 A n P_{eR} C_f \tag{24}$$

where A (=95%) is the availability of the wind power resource for generating electricity. Therefore, the cost of electricity (COE) per unit kW-hr in the PVC method is given by:

$$COE = \frac{PVC}{E_{WT}} \tag{25}$$

3. Results and Discussion

3.1. On the Wind Shear Exponent

All the values of the wind shear exponent (α) obtained in this study lie in the range [0.10; 0.40] in accordance with results from other works [33] [34] [35]. The monthly and annual averages shown in Table 2 indicate that the two sites are weakly windy, since high values of α ($\alpha > \alpha_0 = \frac{1}{7} \approx 0.14$) refer to low wind speed (v) values. Moreover, those results indicate that the two sites should be worded as suburbs and wooded countryside, which refer to between roughness classes 2 and 3 [36] [37].

In mean seasonal trends, the driest months (from August to October) are the windiest (with lowest α or highest v values) at the two sites. Table 3 indicates at its turn that, in mean diurnal trends, the half-day period is windier than the

Table 1. Range of WTs' specific costs (in US $/kW) based on the rated power.

WT size (kW)	Specific costs	Mean specific cost
Less than 20	2200 - 3000	2600
20 - 200	1250 - 2300	1775
200 and above	700 - 1600	1150

Table 2. Monthly and annual mean values of the wind shear exponent (α).

Period	Jan	Feb	Mar	Apr	May	Jun	Jul	Aug	Sep	Oct	Nov	Dec	Year
Bujumbura	0.24	0.23	0.24	0.25	0.27	0.26	0.27	0.23	0.23	0.24	0.24	0.25	0.25
Muyinga	0.25	0.24	0.26	0.29	0.31	0.29	0.30	0.21	0.19	0.18	---	---	0.25

Table 3. Diurnal variations of the wind shear exponent's mean values.

3-hour Period	6:00-9:00	9:00-12:00	12:00-15:00	15:00-18:00
Bujumbura	0.21	0.14	0.17	0.19
Muyinga	0.25	0.15	0.17	0.24

morning and evening periods. This feature has been evidenced in other works [14] [35].

3.2. On the Average Wind Direction

An analysis of the data quoted in Section 2.1 shows that the average wind direction at Bujumbura is north (N) in the morning and south (S) in the afternoon. Nevertheless, the morning wind direction at that site is sometimes (but seldom) S, south-west (SW) or north-west (NW). At the opposite, the average wind direction at Muyinga is S all along the day. The wind direction's inversion phenomenon observed at the midday for Bujumbura should be ascribed to the alternation between the land's breeze and the lake's breeze (that site is located at the border of the Tanganyika lake).

3.3. On the Weibull PDFs Fitting the Observed Relative Frequency Distributions of Wind Speed Data

Table 4(a) and **Table 4(b)** exhibit firstly average ($\overline{v}$) and standard deviation (σ) values of the monthly and annual frequency distributions of wind speed data observed at 12 m height AGL for Bujumbura and Muyinga, respectively. They show secondly values of the shape (k) and scale (c) parameters of the Weibull PDFs fitting those distributions. Finally, values of the variables *MBE*, *RMSE*, t and t_c of the statistical tests performed to measure the effectiveness of the fitting technique, are also given in those tables.

Those results indicate that the frequency distributions of wind speed data are more spread and asymmetrical for Bujumbura than for Muyinga. Their annual mean values are of 3.55 m/s and 1.61 m/s, respectively at 12 m height AGL. The driest months (from August to October) are the windiest in Bujumbura. In Muyinga, the highest mean wind speeds are noticed both in the dry season (July and September) and in the rainy one (April). The Weibull PDFs fitting the observed monthly and annual frequency distributions of wind speed data at the two sites are closer to Rayleigh PDFs than to exponential PDFs, since the shape parameter (k) is closer to 2 than to 1 in most of the cases. Moreover, any of the 26 Weibull PDFs implemented in this study is a very good fit of the related observed frequency distribution of wind speed data. As a matter of fact, for each data set, the *MBE* is found equal (or very close) to zero, the *RMSE* is very low and values of the t-statistics are either equal to zero or much lower than their critical counterparts. **Figure 2** and **Figure 3** illustrate some of those fits for the two sites, respectively.

Table 4. (a). Results of the fitting technique on wind speed data observed at 12 m height AGL for Bujumbura. (b). Results of the fitting technique on wind speed data observed at 12 m height AGL for Muyinga.

(a)

Period	$\overline{v}$ (m/s)	σ (m/s)	k	c (m/s)	*MBE*	*RMSE*	t	t_c
January	3.143	1.616	2.059	3.531	0.0000	0.0348	0.000	3.355
February	2.760	1.330	2.210	3.101	0.0006	0.0517	0.032	3.355
March	3.334	1.813	1.938	3.746	−0.0010	0.0669	0.040	3.355
April	3.412	1.892	1.897	3.834	0.0000	0.0505	0.000	3.250
May	3.471	1.994	1.826	3.900	0.0100	0.0574	0.468	3.355
June	3.602	2.185	1.721	4.047	0.0013	0.0658	0.057	3.250
July	3.817	2.171	1.846	4.289	0.0106	0.0744	0.381	3.355
August	4.194	2.291	1.928	4.712	0.0002	0.0521	0.011	3.106
September	4.067	2.098	2.052	4.570	0.0121	0.0377	0.959	3.250
October	4.090	2.284	1.883	4.596	−0.0001	0.0383	0.007	3.106
November	3.638	2.310	1.638	4.088	0.0008	0.0482	0.052	3.055
December	3.070	1.716	1.881	3.449	0.0000	0.0469	0.000	3.355
Year	3.545	2.026	1.836	3.983	0.0007	0.0415	0.054	3.055

(b)

Period	$\overline{v}$ (m/s)	σ (m/s)	k	c (m/s)	*MBE*	*RMSE*	t	t_c
January	1.709	0.687	2.069	1.920	0.0006	0.0552	0.022	4.032
February	1.466	0.656	2.395	1.647	0.0040	0.0208	0.339	4.604
March	1.732	0.762	2.439	1.946	0.0020	0.0153	0.264	4.032
April	1.849	0.687	2.931	2.078	0.0002	0.0357	0.011	4.032
May	1.734	0.612	3.099	1.927	−0.0005	0.0361	0.024	4.604
June	1.609	0.681	2.544	1.808	−0.0037	0.0396	0.133	5.841
July	1.925	0.753	2.771	2.163	0.0003	0.0342	0.013	4.604
August	1.531	0.646	2.553	1.720	0.0025	0.0263	0.166	4.604
September	1.811	0.763	2.557	2.035	0.0005	0.0239	0.036	4.604
October	1.499	0.792	1.999	1.684	0.0075	0.0486	0.271	4.604
November	1.226	0.742	1.725	1.378	0.0143	0.0358	0.751	4.604
December	1.234	0.719	1.798	1.387	0.0188	0.0513	0.680	4.604
Year	1.611	0.742	2.321	1.810	−0.0040	0.0154	0.601	3.707

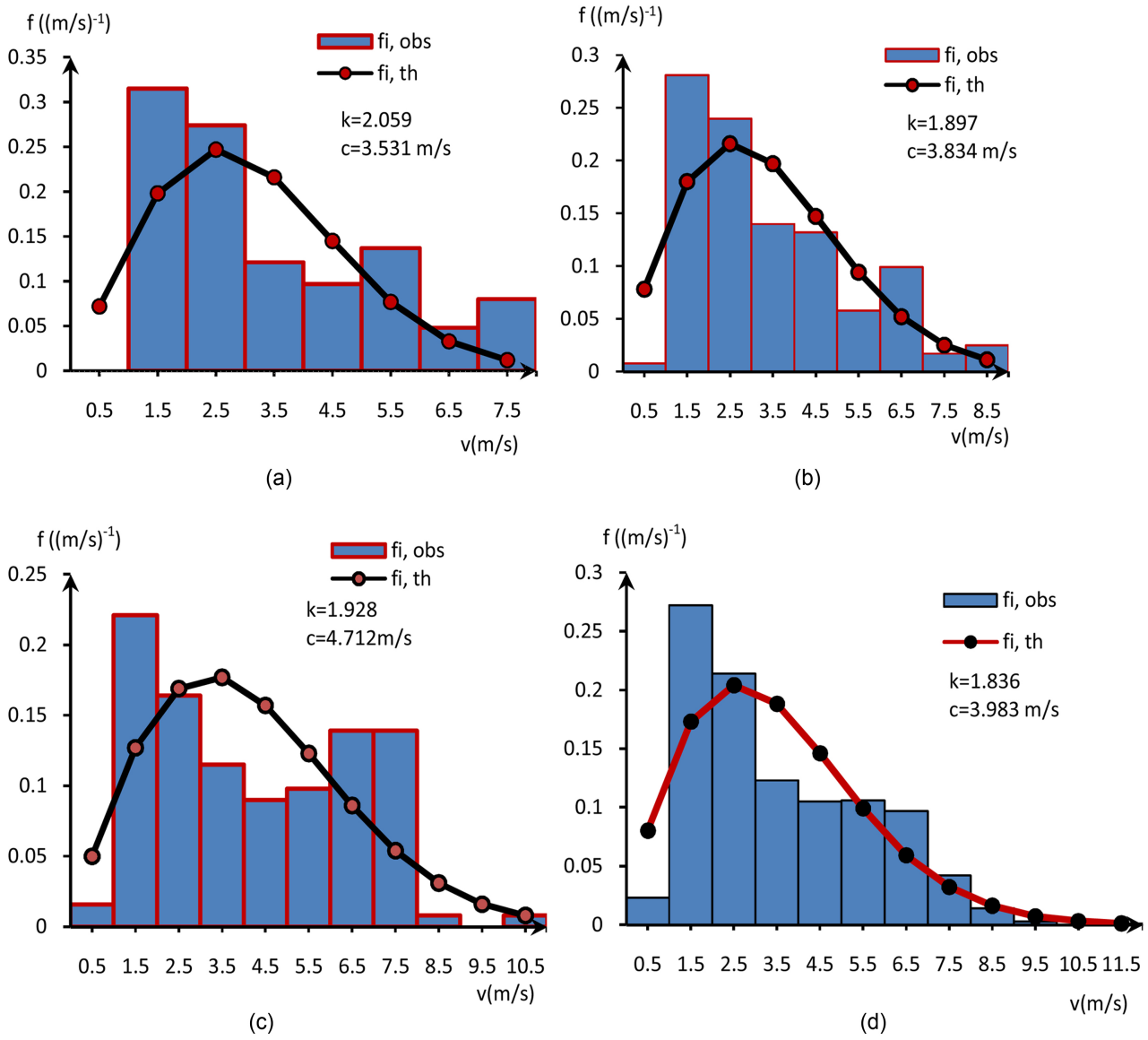

Figure 2. Observed monthly and annual relative frequency distributions ($f_{i,obs}$) of wind speed data and Weibull PDFs ($f_{i,th}$) fitting them for Bujumbura, at 12 m height AGL. (a) January; (b) April; (c) August; (d) year.

3.4. On the Wind Power and Energy Content

The average wind speed ($\overline{v}$), Weibull shape and scale parameters (k and c), power and energy densities ($\overline{p}$ and $\overline{e}$), energy pattern factor (E_{PF}), most probable and optimum wind speeds (v_{mp} and v_{op}) at reference height z_0 = 10 mAGL are summarized in Table 5(a) and Table 5(b) for the two sites of this analysis.

Those results show that the mean wind speed and power (or energy) density have similar changing trend, but with different rates of change. As a matter of fact, the power (or energy) density depends not only on the wind speed, but also on the shape parameter k. It is also observed that, in decreasing order, August, October, September, July, November and June are the six months which exhibit

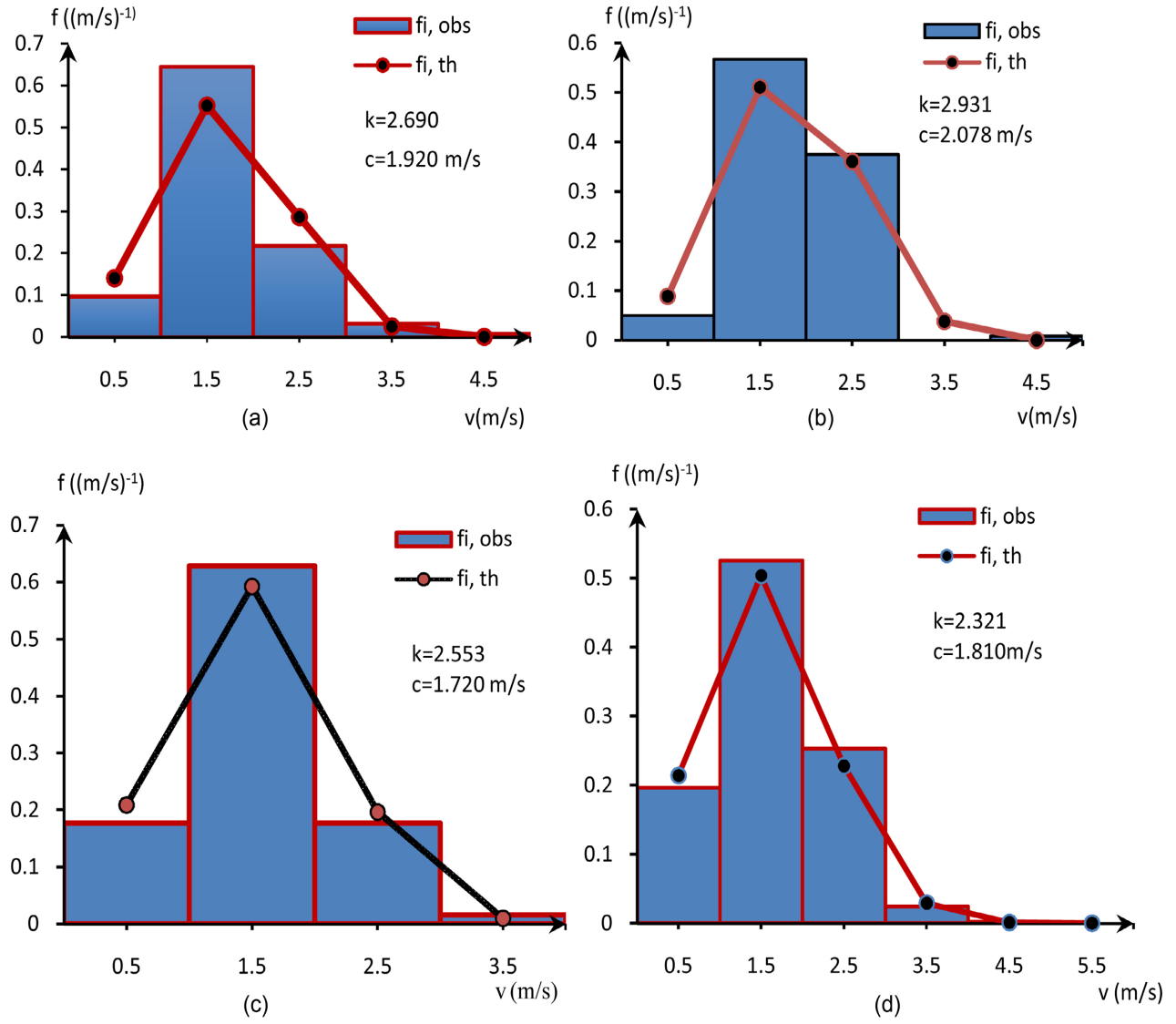

Figure 3. Observed monthly and annual relative frequency distributions ($f_{i,obs}$) of wind speed data and Weibull PDFs ($f_{i,th}$) fitting them for Muyinga, at 12 m height AGL. (a) January; (b) April; (c) August; (d) year.

the highest wind power (or energy) potential at Bujumbura. In the same kind of order, the six months with the highest wind power (or energy) potential at Muyinga are July, September, April, March, January and May. Nevertheless, the annual mean wind power (or energy) density at reference height AGL is about thirteen fold greater at Bujumbura than at Muyinga.

3.5. On the Use and Performance of Selected Wind Machines

3.5.1. At Small, Individual Scale

Following the Pacific Northwest National Laboratory's classification of sites according to their annual mean wind speed and power density [38], at 10 m height AGL, any of the two sites of this study falls under class 1 and is an unsuitable location for generating electricity. Instead of direct electricity production, the wind

Table 5. (a). Monthly and annual wind characteristics at 10 m height AGL, for Bujumbura. (b). Monthly and annual wind characteristics at 10 m height AGL, for Muyinga.

(a)

Period	$\overline{v}$ (m/s)	k	c (m/s)	$\overline{p}$ (W/m^2)	$\overline{e}$ (kW-hr/m^2)	E_{PF}	v_{mp} (m/s)	v_{op} (m/s)
Jan	3.003	2.059	3.374	30.113	20.40	1.83	2.443	4.691
Feb	2.627	2.210	2.963	19.120	13.31	1.72	2.256	3.966
Mar	3.185	1.938	3.579	38.750	28.83	1.96	2.461	5.160
Apr	3.260	1.897	3.663	42.446	30.56	2.00	2.468	5.354
May	3.316	1.826	3.726	46.892	34.89	2.10	2.413	5.587
Jun	3.442	1.721	3.867	56.667	40.80	2.27	2.333	6.053
Jul	3.647	1.846	4.098	61.542	45.79	2.07	2.805	6.099
Aug	4.007	1.928	4.502	77.685	57.80	1.97	3.081	6.512
Sept	3.886	2.052	4.366	65.758	47.35	1.83	3.153	6.083
Oct	3.908	1.883	4.391	73.635	54.78	2.01	2.937	6.449
Nov	3.476	1.638	3.906	62.781	45.20	2.44	2.197	6.358
Dec	2.933	1.881	3.296	31.362	23.33	2.03	2.202	4.844
Year	3.387	1.836	3.806	49.640	436.04	2.09	2.480	5.685

(b)

Period	$\overline{v}$ (m/s)	k	c (m/s)	$\overline{p}$ (W/m^2)	$\overline{e}$ (kW-hr/m^2)	E_{PF}	v_{mp} (m/s)	v_{op} (m/s)
Jan	1.633	2.690	1.834	3.967	2.95	1.50	1.543	2.255
Feb	1.401	2.395	1.574	2.699	1.88	1.60	1.256	2.028
Mar	1.655	2.439	1.859	4.407	3.28	1.59	1.497	2.124
Apr	1.767	2.931	1.985	4.838	3.48	1.43	1.722	2.370
May	1.657	3.099	1.841	3.784	2.82	1.40	1.624	2.162
Jun	1.537	2.544	1.727	3.439	2.48	1.55	1.419	2.169
Jul	1.839	2.771	2.067	5.625	4.19	1.48	1.759	2.515
Aug	1.463	2.553	1.643	2.961	2.20	1.55	1.352	2.061
Sept	1.730	2.557	1.944	4.875	3.51	1.55	1.601	2.437
Oct	1.432	1.999	1.609	3.393	2.52	1.89	1.137	2.276
Nov	1.171	1.725	1.317	2.239	1.61	2.27	0.797	2.058
Dec	1.179	1.798	1.325	2.151	1.60	2.14	0.843	2.008
Year	1.539	2.321	1.729	3.717	32.65	1.65	1.356	2.260

energy potential at those sites is high enough to power simple machines of less than 5 kW in rated power capacity. Those machines could be associated with full energy charging and storage in chemical storage batteries, together with load distributors for individual premises. Through those distributors, the energy extracted from the wind would be channeled into different useful purposes in the dwellings and barns. The use of those machines in water pumping for irrigation would be an alternative to battery storage [39]. This feature would be particularly relevant for the agricultural area localities in the surroundings of the data collection station of Bujumbura, where the dry season encloses the windiest months of the year. For all those purposes, simple and inexpensive locally manufactured designs having very low cut-in wind speeds (<2 m/s) and which can withstand high wind gusts (>25 m/s), could be used.

3.5.2. At Medium and Large Scales

From the 10 m AGL data of **Table 5(a)** and **Table 5(b)**, power law of Equation (10) and Equation (11) for the wind power density, have been used to extrapolate annual average wind speed and wind power density at different WT hub heights. For Bujumbura, an extrapolation to 150, 200, 250, 300 and 350 m AGL, which represent selected exposed ridge-tops and hilltops around the data collection station, has led to mean wind speeds from 6.67 to 8.24 m/s and mean wind power densities from 375.36 to 714.30 W/m^2. Those results indicate that the above-mentioned ridge-tops and hilltops fall under wind classes from 3 to 6, and that their wind energy potential is therefore deemed suitable for medium and large scale electricity production. An extrapolation for Muyinga at the same heights AGL has given mean wind speeds from 3.03 to 3.74 m/s and mean power densities from 28.33 to 53.49 W/m^2. Those features, which refer to wind sites of class 1, indicate that the wind energy potential of ridge-tops and hilltops around Muyinga data collection station is unsuitable for medium and large electricity generation. Instead of that, small and individual scale wind energy applications such as those described in sub-section 3.5.1 should be foreseen for that locality.

As shown in **Table 6**, ten WTs have been selected for possible installation at the above-mentioned sites around Bujumbura. All of them have pitch control system, with rated power ranging from 9.7 to 3000 kW, hub heights between 25 and 80 m, and power curves as provided in the relevant references (cited websites) [40]-[47].

Annual average power and energy outputs, capacity factors, together with average costs of electricity's estimates of those selected WTs at exposed ridge-tops and hilltops in the surroundings of Bujumbura, are shown in **Table 7**, where E_{out} is the WT's energy output during one year.

The top five highest capacity factors are observed using P15-50 (50 kW), P25-100 (100 kW), P12-25 (25 kW), YDF-1500-87 (1500 kW) and S95-2.1 MW WTs, while V47-600 (600 kW) and V90-3 MW exhibit the lowest capacity factors. In the meantime, the lowest costs of electricity are noticed with large WTs

Table 6. Characteristics of selected wind turbines.

WT	Hub height (m)	Rated power (kW)	Diameter (m)	Cut-in wind speed (m/s)	Rated wind speed (m/s)	Cut-out wind speed (m/s)
AOC Windlite10 kW DC WT	25	9.7	7.0	4.0	10.5	18
P10-20	36.6	20	10	2.7	11.0	25
P15-50	50	50	15.2	2.5	10.0	25
P25-100	45.7	100	25.0	2.7	10.0	25
Enercon E-33	50	330	33.4	2.5	13	28
Vestas V-47 660 KW	45	660	47	4.5	14	25
Enercon E-48	70	800	50	3.0	14	25
YDF-1500-87	75	1500	87	3	10.2	25
S95-2.1 MW	80	2100	95.0	3.5	11.0	25
Vestas V90 3 MW	80	3000	90	3.5	15	25

Table 7. Performance of selected WTs and cost of electricity at hilltops around Bujumbura.

WT	Hilltop (m AGL)	Hub height (m)	P_{eR} (kW)	$P_{e,ave}$ (kW)	C_f (%)	E_{out} (MW-hr/yr)	COE (US $/kW-hr)
AOC/10 kW	150	37	9.7	3.74	38.59	31.12	0.169
	350	37	9.7	3.75	38.69	31.21	0.169
P12-25	150	36.6	25	10.48	41.92	87.21	0.106
	350	36.6	25	14.23	56.92	118.42	0.078
P15-50	150	50	50	24.19	48.36	201.31	0.092
	350	50	50	28.86	57.72	240.17	0.077
P25-100	150	45.7	100	47.52	47.52	395.46	0.094
	350	45.7	100	57.22	57.22	476.18	0.078
E-33/330	150	50	330	115.06	34.87	957.53	0.082
	350	50	330	147.12	44.58	1224.33	0.065
V47-660	150	45	660	173.97	26.33	1447.78	0.110
	350	45	660	195.36	29.60	1625.79	0.098
E48-800	150	70	800	251.76	31.47	2095.15	0.092
	350	70	800	321.89	40.24	2678.77	0.072
YDF-1500	150	75	1500	761.48	47.72	6337.04	0.057
-87	350	75	1500	862.91	56.86	7181.14	0.050
S95-2.1 MW	150	80	2100	899.81	42.85	7488.22	0.067
	350	80	2100	1087.55	51.79	9050.59	0.056
V90-3 MW	150	80	3000	834.76	27.83	6946.87	0.104
	350	80	3000	1082.17	36.07	9005.82	0.080

(YDF-1500-87 and S95-2.1 MW), while small WTs (P15-50, P25-100 and P12-25) show very good capacity factors, but higher costs of electricity when compared to large WTs.

Within the setting on ridge-tops and hilltops 150 m AGL around Bujumbura, YDF-1500-87 should be selected owing to its high capacity factor and low cost of electricity. These quantities have been computed on monthly basis and results are shown in Figure 4.

The minimum capacity factor (33.01%) and maximum cost of electricity (0.094 US $/kW-hr) occur simultaneously in February. At the opposite, the highest capacity factors (with maximum of 56.96% in August) and the lowest costs of electricity (with minimum of 0.050 US $/kW-hr in the same month) are observed in the dry season (from June to November). From Figure 4, it is shown that any increase of the CF occurs simultaneously with a decrease of the COE. At the opposite, when the CF decreases, the COE increases. Those features are well in accordance with the relationships (21) and (25) defining the CF and the COE, respectively. As a matter of fact, in those equations, the rated electrical power (P_{eR}))and the present value of cost (PVC; Equation (22)) are unchanging parameters for a given WT. At the opposite, the WT's average electrical power output ($P_{e,ave}$; Equation (20)) and the WT's total energy output (E_{WT}; Equation (24)) are changing quantities which exhibit the same seasonal variations.

The average monthly household hydroelectricity consumption in Burundi is 150 kW-hr for a present cost of 33,100 BIF (local currency). As the present local rate of exchange ranges from 2200 BIF (official rate) to 3400 BIF (black market rate) for 1 US $, that means a local average COE (hydroelectricity) which ranges from 0.065 to 0.100 US $/kW-hr. A comparison of those features with COE data from Table 7 and Figure 4 leads to the following evidence: the option of installing

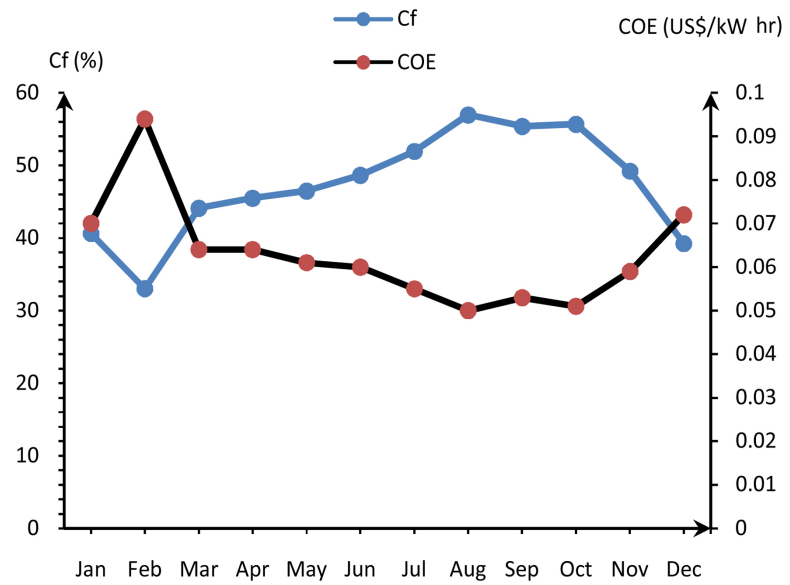

Figure 4. Monthly variations of YDF-1500-87 WT's capacity factor and cost of electricity at hilltops 150 m around Bujumbura.

WECS as clean energy sources in order to supplement traditional ones is economically feasible in well selected Burundian sites. That should be particularly beneficent in reducing electricity shortages commonly observed in different localities, especially during the dry season. Those WECS should be planned for not only onshore setting, but also for offshore setting, for example in the Tanganyika lake and other lakes in the North-East region of the country.

4. Conclusions

The present wind resource analysis for Bujumbura and Muyinga has led to the following results. The average shear exponent is 0.25 at any of those sites. The driest months are the windiest, and the half-day period is windier than the morning and evening periods. The average wind direction at Muyinga is south all along the day, while average wind directions at Bujumbura are north in the morning and south in the afternoon. Since Bujumbura is located near the Tanganyika lake, that midday inversion phenomenon should be ascribed to the alternation between the land's and lake's breezes.

All the 26 two-parameter Weibull PDFs implemented to fit the related observed monthly and annual relative frequency distributions of wind speed data at the two sites, have been found very satisfactory as exhibited through three complementary statistical tests. The average wind power density at 10 m AGL is about thirteen fold higher at Bujumbura than at Muyinga. Hilltops located from 150 to 350 m AGL around Muyinga are wind sites of class 1, where only small, individual scale WECS should be installed.

At the same heights AGL, exposed ridge-tops and hilltops in the surroundings of Bujumbura are contrarily wind sites of classes from 3 to 6, which are suitable for medium and large scale electricity generation.

Amongst ten WTs (with rated capacity ranging from 9.7 to 3000 kW and hub heights between 25 and 80 m) selected for possible installation at the previous ridge-tops and hilltops, YDF-1500-87 and S95-2.1 MW have emerged as the best candidates owing to their highest capacity factors and lowest costs of electricity per unit energy output. From a monthly basis analysis, it has also been shown that the best performance of YDF-1500-87 WT is observed during the dry season (from June to November), with maximum capacity factor (56.96%) and minimum cost of electricity (0.050 US $/kW-hr) in August. Furthermore, the analysis has evidenced economical feasibility and benefit of setting WECS in selected Burundian sites in order to supplement traditional electricity sources.

Acknowledgements

The authors gratefully acknowledge the IGEBU weather service (Gitega) for having kindly provided them with the basic data used in this work.

Conflicts of Interest

The authors declare no conflicts of interest regarding the publication of this paper.

References

[1] Plan National de Développement (PND Burundi 2018-2027) (2018, August 31) Annexe 2. 73-87. https://www.presidence.gov.bi/wp-content/uploads/2018/08/PND-Burundi-2018-2027-Version-Finale.pdf

[2] International Rankings of Burundi—2017; Burundi Data Portal. https://burundi.opendataforafrica.org/data#menu=topic

[3] Complete Vision Burundi 2025 (June 2011). https://www.presidence.gov.bi/archives/IMG/pdf/Vision_Burundi_2025_complete_FR.pdf

[4] République du Burundi, Cadre Stratégique de Croissance et de Lutte contre la Pauvreté, CSLP II: 2012-2015, Bilan de Mise en Œuvre. https://www1.undp.org/content/dam/burundi/docs/publications/Rapport Bilan global du CSLPII_final.pdf

[5] Mathews, S., Pandey, K.P. and Kumar, A.V. (2002) Analysis of Wind Regimes for Energy Estimation. *Renewable Energy*, **25**, 381-399. https://doi.org/10.1016/S0960-1481(01)00063-5

[6] Karsli, V.M. and Geçit, C. (2003) An Investigation on Wind Power Potential of Nurdağı-Gaziantep, Turkey. *Renewable Energy*, **28**, 823-830. https://doi.org/10.1016/S0960-1481(02)00059-9

[7] Teez, H.W., Harms, T.M. and Von Backström, T.W. (2003) Assessment of the Wind Power Potential at SANAE IV Base, Antarctica: A Technical and Economic Feasibility Study. *Renewable Energy*, **28**, 2037-2061. https://doi.org/10.1016/S0960-1481(03)00076-4

[8] Toledo Velásquez, M., Hernández Rodriguez, J., Vega Del Carmen, M., Flores Murrieta, F.E. and Tolentino Eslava, G. (2016) Application of the Weibull Distribution to Estimate the Volume of Water Pumping by a Windmill. *Journal of Power and Energy Engineering*, **4**, 36-51. https://doi.org/10.4236/jpee.2016.49004

[9] Kazet, M.Y., Mouangue, R., Kuitche, A. and Ndjaka, J.M. (2016) Wind Energy Resource Assessment in Ngaoundere Locality. *Energy Procedia*, **93**, 74-81. https://doi.org/10.1016/j.egypro.2016.07.152

[10] Boudia, S.M., Berrached, S. and Bouri, S. (2016) On the Use of Wind Energy at Tlemsen, North-Western Region of Algeria. *Energy Procedia*, **93**, 141-145. https://doi.org/10.1016/j.egypro.2016.07.162

[11] Gatoto, P., Lollchund, M.R. and Dalson, G.A. (2021) Wind Energy Potential Assessment of Some Sites in Burundi Using Statistical Modeling. *Proceedings of* 2021 *IEEE PES/IAS Power Africa Virtual Conference*, Nairobi, 23-27 August 2021, 219-223.

[12] Ayala, M., Maldonado, J., Paccha, E. and Riba, C. (2017) Wind Power Resource Assessment in Complex Terrain: Villonaco Case-Study Using Computational Fluid Dynamics Analysis. *Energy Procedia*, **107**, 41-48. https://doi.org/10.1016/j.egypro.2016.12.127

[13] Ilinca, A., McCarthy, E., Chaumel, J.-L. and Rétiveau, J.-L. (2003) Wind Potential Assessment of Quebec Province. *Renewable Energy*, **28**, 1881-1897. https://doi.org/10.1016/S0960-1481(03)00072-7

[14] Farrugia, R.N. (2003) The Wind Shear Exponent in a Mediterranean Island Climate. *Renewable Energy*, **28**, 647-653. https://doi.org/10.1016/S0960-1481(02)00066-6

[15] Chang, T.-J., Wu, Y.-T., Hsu, H.-Y., Chu, C.-R. and Liao, C.-M. (2003) Assessment of Wind Characteristics and Wind Turbine Characteristics in Taiwan. *Renewable*

Energy, **28**, 851-871. https://doi.org/10.1016/S0960-1481(02)00184-2

[16] Al-Mahamad, A. and Karmeh, H. (2003) Wind Energy Potential in Syria. *Renewable Energy*, **28**, 1039-1046. https://doi.org/10.1016/S0960-1481(02)00186-6

[17] Ayik, A. , Ijumba, N., Kabiri, C. and Goffin, P. (2021) Preliminary Wind Resource Assessment in South Sudan Using Reanalysis Data and Statistical Methods. *Renewable and Sustainable Energy Reviews*, **138**, Article ID: 110621. https://doi.org/10.1016/j.rser.2020.110621

[18] Azad, K., Rasul, M., Halder, P. and Sutariya, J. (2019) Assessment of Wind Energy Prospect by Weibull Distribution for Prospective Wind Sites in Australia. *Energy Procedia*, **160**, 348-355. https://doi.org/10.1016/j.egypro.2019.02.167

[19] Parajuli, A. (2016) A Statistical Analysis of Wind Speed and Power Density Based on Weibull and Rayleigh Models of Jumla, Nepal. *Energy and Power Engineering*, **8**, 271-282. https://doi.org/10.4236/epe.2016.87026

[20] Galarza, J. (2021) Assessment of Wind Energy Potential and the Application for Microturbines. *International Journal of Electrical Engineering and Technology* (*IJEET*), **12**, 20-31. https://doi.org/10.34218/IJEET.12.9.2021.003

[21] Nielsen, M.A. (2011) Parameter Estimation for the Two-Parameter Weibull Distribution. Brigham Young University, Provo, 7-31. http://scholarsarchive.byu.edu/etd

[22] Lu, L., Zang, H. and Barnett, J. (2002) Investigation on the Wind Power Potential on Hong Kong Islands: An Analysis of Wind Power and Wind Turbine Characteristics. *Renewable Energy*, **27**, 1-12. https://doi.org/10.1016/S0960-1481(01)00164-1

[23] Weisser, D. (2003) A Wind Energy Analysis of Grenada: An Estimation Using the Weibull Density Function. *Renewable Energy*, **28**, 1801-1812. https://doi.org/10.1016/S0960-1481(03)00016-8

[24] Gamma Function $\Gamma(n)$ Table. https://getcalc.com/statistics-gamma-function-table.htm

[25] Bashahu, M. (2003) Statistical Comparison of Models for Estimating the Monthly Average Daily Diffuse Radiation at a Subtropical African Site. *Solar Energy*, **75**, 43-51. https://doi.org/10.1016/S0038-092X(03)00213-5

[26] Bashahu, M. and Mpanzimana, D. (2009) Estimation of the Monthly Average Daily Solar Global Irradiation with Climatological Parameters at Some Burundian Stations. *International Review of Physics*, **3**, 237-243.

[27] Bashahu, M. and Buseke, M. (2016) Statistical Analysis of Hourly Wind Speed Data from Burundian Stations Using Beta Probability Density Functions. *Modern Environmental Science and Engineering*, **2**, 740-746. https://doi.org/10.15341/mese(2333-2581)/11.02.2016/005

[28] Bashahu, M. and Ntirandekura, J. (2018) Statistical Analysis of Hourly Clearness Index and Diffuse Fraction Data Using Beta Probability Density Functions. *Modern Environmental Science and Engineering*, **4**, 350-357.

[29] Honercamp, J. (1999) Stochastic Dynamical Systems: Concepts, Numerical Methods, Data Analysis. VHC Publishers, Weinheim, 511.

[30] Critical Values of Student's *t* Distribution with ν Degrees of Freedom (t_{1-a}, ν). https://www.itl.nist.gov/div898/handbook/eda/section3

[31] Kidmo, D.K., Deli, K., Raidandi, D. and Yaminyo, S.D. (2016) Wind Energy for Electricity Generation in the Far North Region of Cameroon. *Energy Procedia*, **93**, 66-73. https://doi.org/10.1016/j.egypro.2016.07.151

[32] Gaddada, S. and Kodicherla, S.P.K. (2016) Wind Energy Potential and Cost Estimation of Wind Energy Conversion Systems for Electricity Generation in the Eight Se-

lected Locations of Tigray Region (Ethiopia). *Renewables: Wind, Water and Solar*, **3**, Article No. 10. https://doi.org/10.1186/s40807-016-0030-8

[33] Legourières, D. (1980) Energie Eolienne: Théorie, Conception et Calcul Pratique des Installations.Eyrolles, Paris, 7-17.

[34] Park, J. (1981) The Wind Power Book. Cheshire Books, Fort Bragg, 49-55, 164.

[35] Altaii, K. and Farrugia, R.N. (2003) Wind Characteristics on the Caribbean Island of Puerto Rico. *Renewable Energy*, **28**, 1701-1710. https://doi.org/10.1016/S0960-1481(03)00039-9

[36] Burton, T., Sharpe, D., Jenkins, N. and Bossanyi, E. (2001) Wind Energy Handbook. Wiley, Hoboken, 19. https://doi.org/10.1002/0470846062

[37] D'Ambrosio, M. and Medaglia, M. (2010) Vertical Axis Wind Turbines: History, Technology and Applications. Högskolan-Halmstad, Halmstad, 27.

[38] Classes of Wind Power Density at 10 m and 50 m, Table 1-1, p. 1.

[39] Energy and Power Content of the Wind, M. Ragheb, pp. 3, 12-15. http://mragheb.com

[40] CNYD YDF-1500-87 Description, Wind Turbines. https://en.wind-turbine.com/wind-turbine/11328/enyd-ydf-1500-87.html

[41] E33/660 (Enercon), Wind Power. https://www.thewindpower.net/turbine_en_1_enercon_e33-330.php

[42] E48/800 (Enercon), Wind Power. https://www.thewindpower.net/turbine_en_3_enercon_e48-800.php

[43] Preliminary Design Specifications for the Windlite 10 kW DC Generator, March 2000. https://www.researchgate.net/figure/WindLite-Rotor-Characteristics_tbl1_242076882

[44] S95-2.1 MW Technical Specifications. Suzlon Energy Ltd., Annex 8, pp. 1-18. https://www.thewindpower.net/turbine_en_766_suzlon_s95-2100.php

[45] Specification Sheets for the P10-20, P12-25, P15-50 and P25-10 Wind Turbines. Polaris America LLC. http://www.polarisamerica.com/turbines/technology

[46] V47/660 (Vestas), Wind Power. https://www.thewindpower.net/turbine_en_176_vestas_v47-660.php

[47] V90-3.0 MW General Specification. Vestas Wind Systems A/S, 2004, pp. 1-31.